

4.2 Experiments at the 12 GeV Proton Synchrotron

The KEK 12 GeV Proton Synchrotron (PS) was operated in slow beam-extraction mode in April, May, and June. After the summer shutdown, fast beam-extraction mode was started at the end of September and was scheduled to be continued until the end of FY2004. Due to an electrical fault of the first horn of the neutrino beam line in November, however, data acquisition from the K2K experiment (E362) was halted and the initial plan was switched over to accelerator study and R&D of detectors for J-PARC and the next-generation long-baseline neutrino oscillation experiment (T2K) until the end of December. Accelerator operation was then changed to the slow beam-extraction mode in January, February, and March. During the period in slow beam-extraction mode, about 4.5 months in total, work was carried out on the E391a experiment and 18 tests were performed.

E391a is searching for $K_L \rightarrow \pi^0 \nu \bar{\nu}$ decay, which is the most attractive flavor-changing neutral current (FCNC) process in the CP violation study. Since the decay probability is well calculated with a negligible ambiguity in the Standard Model (SM), it provides the cleanest test of the SM and any deviation from the expectation will be a clear signal of the new physics. The experiment performed data taking successfully for 100 days from February to June 2004. During the data taking, it was confirmed that the pencil K_L beam and the detector system including the vacuum worked properly as designed. Figure 4-2-1 shows a final plot of prompt analysis using 2% of the obtained data. With such a small fraction of data, the experiment already reaches a sensitivity close to the current experimental limit. In addition to a detailed analysis with higher statistics, a second data taking was performed as an extension for 45 days from February to March 2005 with a few upgrades of the detector system induced by the prompt analysis.

Test experiments were carried out for calibrations and R&D of detectors, preparations for PS experiments, other laboratories, and future facilities. The T535 group verified a novel concept for space-based antimatter detection: the Gaseous Antiparticle Spectrometer (GAPS) employed in the π^2 beam line, as shown in Fig. 4-2-2. The GAPS gas target is designed so that antiprotons with kinetic energy below 100 MeV will be captured into exotic atoms with nearly unity probability. Its detection rates and efficiencies as inferred from an

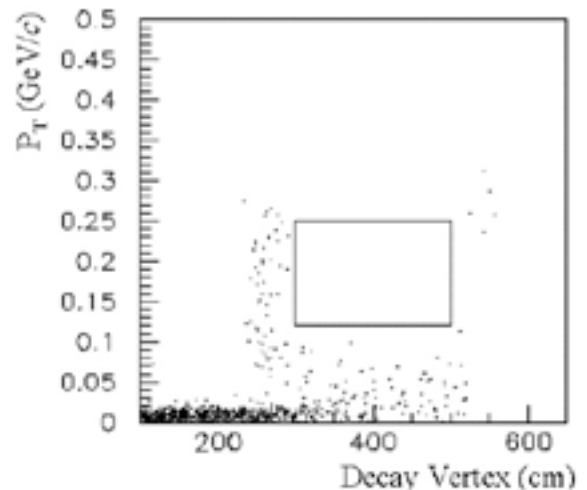


Fig. 4-2-1 Decay vertex versus transverse momentum distribution of reconstructed π^0 from two detected gammas. The rectangular box indicates the signal region searched for $K_L \rightarrow \pi^0 \nu \bar{\nu}$ events. The events surrounding the signal box were identified after a preliminary background analysis as $K_L \rightarrow \gamma \gamma$ decays around $P_T = 0$, events due to interaction of beam particles with upstream (vertex = 300 cm) and downstream (vertex = 550 cm) detectors, and events from several sources including K_L decays at lower P_T below the signal box.



Fig. 4-2-2 Photograph of the GAPS detector with the gas target in the π^2 beam line.

experiment with 27 antiprotons per spill are consistent with simulations. The T543 group checked OPERA emulsion films prepared in the Tono mine (Gifu, Japan). Some of the films were picked up and exposed in the T1 beam line to monitor uniformity of refresh performance, sensitivity (grain density), noise (fog), etc. The T553/T577 group tested the tracker based on scintillating fibers for the international Muon Ionization Cooling Experiment (MICE) at RAL, to optimize the concentration of 3HF to the sensitivity of VLPC. The T554 group for (e, e'K⁺) Λ -hypernuclei spectroscopy at the Jefferson Lab investigated the amino-G-salt concentration of water Cerenkov counters so as to have good K⁺ selection at the trigger level. The T555 group evaluated the performance of a Hadron Blind Detector (HBD) and a Time Projection Chamber (TPC) using Gas Electron Multipliers (GEMs) for the PHENIX detector to reduce the background. The T558 group tested the performance of a small prototype TPC (25 cm drift length) with a Multi-Wire Proportional Chamber (MWPC) readout endplate, which was built by MPI Munich and DESY, at the π 2 beam line with 1 tesla in the superconductive solenoidal magnet. The purpose of T561 was R&D of a new gaseous time-of-flight detector: the Multi-gap Resistive Plate Chamber for the PHENIX experiment at RHIC. The T562 group tested a proximity focusing ring imaging Cerenkov (RICH) detector, with a radiator of two or more aerogel layers of different refractive indices. The Cerenkov angle distribution

(Fig. 4-2-3) for the defocusing dual-radiator RICH shows two rings clearly separated from each other. The T564 group studied the readout of a 3-by-3 array of lead-tungstate EM-calorimeters using an avalanche photodiode. The energy resolution for 1 GeV electrons was evaluated to be $\sigma/E = 5.3\%$, including a considerable amount of intrinsic beam-momentum spread of around 3%. The T565 group has been studying a high-resolution time-of-flight counter consisting of a quartz radiator, a micro-channel plate photomultiplier tube (MCP-PMT), and

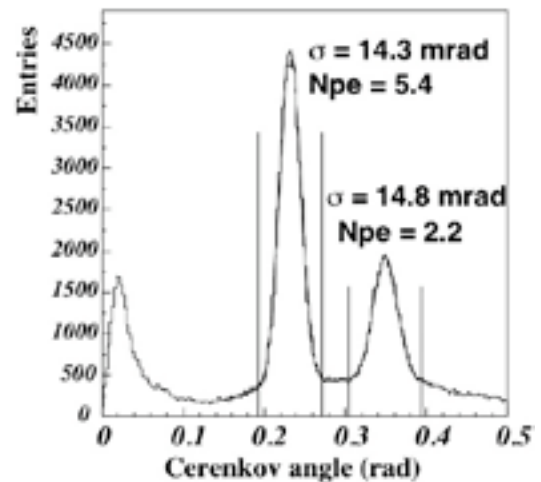


Fig. 4-2-3 Distribution of the Cerenkov angle for accumulated single photons for defocusing dual-radiator RICH using two-layer aerogel.

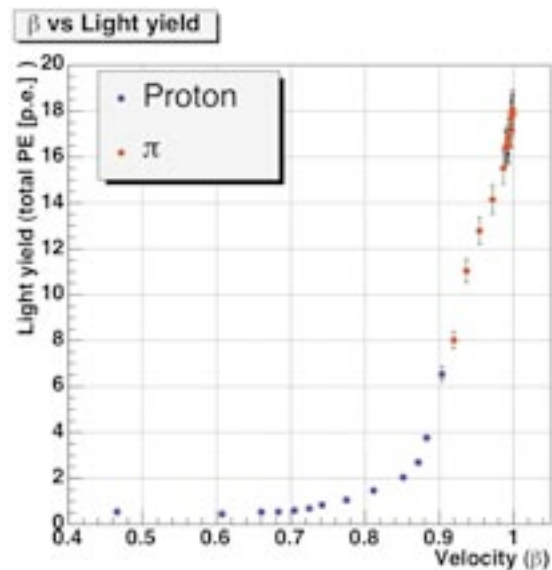
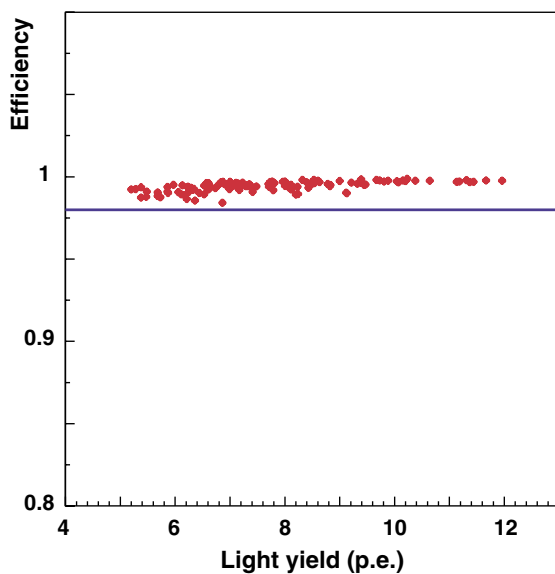


Fig. 4-2-4 (Left) Efficiency versus light yield for one segment of the segmented scintillator tracker. The horizontal line shows 98% efficiency, which was the initial goal of the detector. (Right) Light yield of the acrylic Cerenkov detector as a function of particle velocity.

tungsten plate. The purpose of T568 was irradiation testing of a poly-switch that is expected to have radiation-hardness to fast neutrons. There was no problem in the operation of the poly-switch after 10 days of irradiation (10^{18} primary protons) at the target station of the neutrino beam line. The primary purpose of the T574 experiment was to test a prototype of the range counter and a drift chamber with a large effective area for the E559 experiment, which will study Θ^+ pentaquarks through the reaction $K^+p \rightarrow \Theta^+\pi^+$. The stop positions of the incident particles inside the prototype range counter were consistent with simulations. Also, the efficiencies of the drift chamber and the aerogel counter were confirmed to be high enough. The purpose of experiment T575 is to evaluate prototypes for near detectors in the T2K experiment at J-PARC. Two types of detectors for the on-axis detector, which will monitor the direction of the neutrino beam, were tested: one is a tracker made of plastic scintillator bars, and the other is a Cerenkov detector made from acrylic plate. The results of light yield measurements are shown in Fig. 4-2-4.

Several physics experiments are in the analysis stage. The basic experimental concept of E325 is to measure the modification of spectral functions of vector mesons, which are produced and decay in a nucleus, through invariant mass spectroscopy in the electron-positron pair channel. Detailed analysis has already been carried out for the ϕ meson. The preliminary data shown in Fig. 4-2-5 indicate modification of ϕ 's in the copper target, especially for those that move slowly in the laboratory frame. The observed difference between

carbon and copper targets might be due to the much longer lifetime of the ϕ meson compared to the nuclear radii, leading to different in-medium decay rates. Experiment E471 was performed at K5, using the absorption-reaction of the negative kaon at rest in a helium-4 target. A totally new object of the K^-pnn system named the strange-tribaryon S^0 has been discovered, as shown in Fig. 4-2-6. The E518 group has investigated the precise structure of ${}^1_\Lambda B$ hypernuclei by a high-resolution γ -spectroscopy technique using a large germanium detector array, Hyperball. Six γ transitions

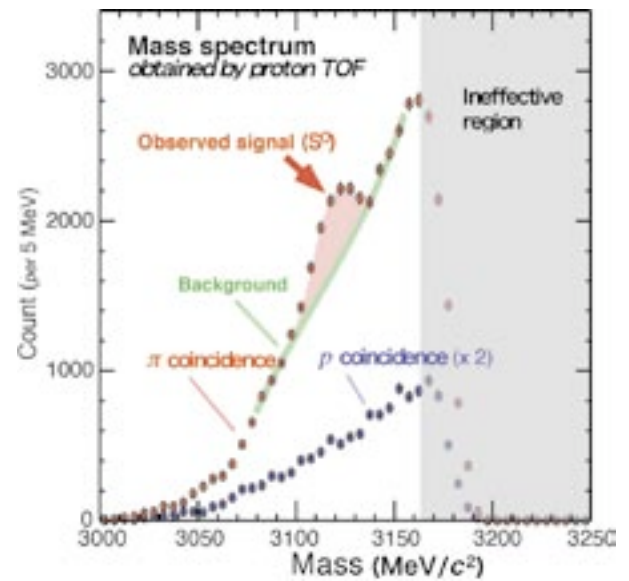


Fig. 4-2-6 Missing mass spectra of the ${}^4\text{He}(\text{stopped } K^-, p)S^0$ reaction, obtained by time-of-flight analysis of the emitted proton.

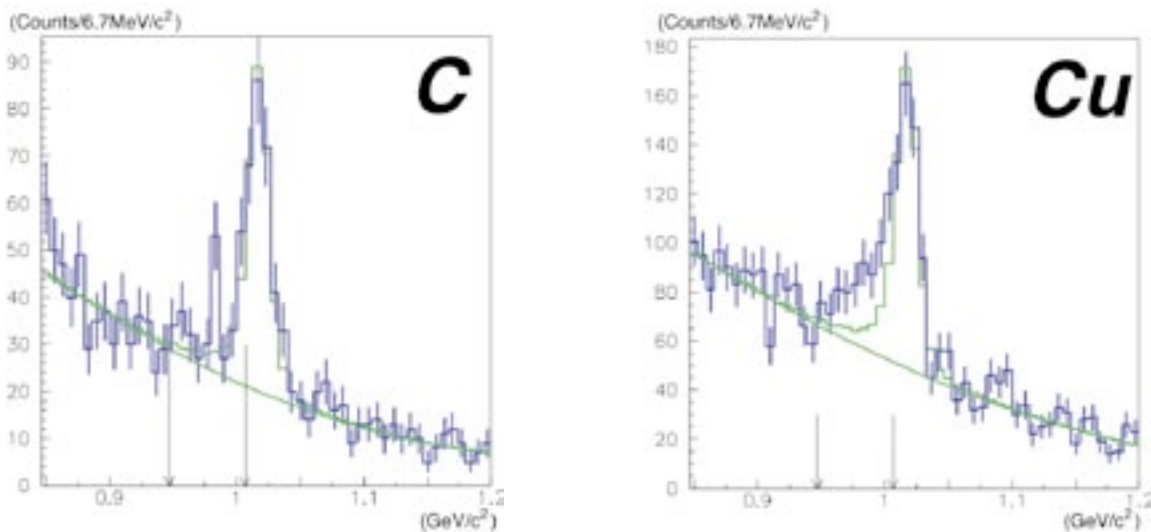


Fig. 4-2-5 Preliminary invariant mass spectra for ϕ , whose $\beta\gamma$ is less than 1.35, for carbon (left) and copper (right) targets. The green histograms are the expected mass shapes due to the detector response.

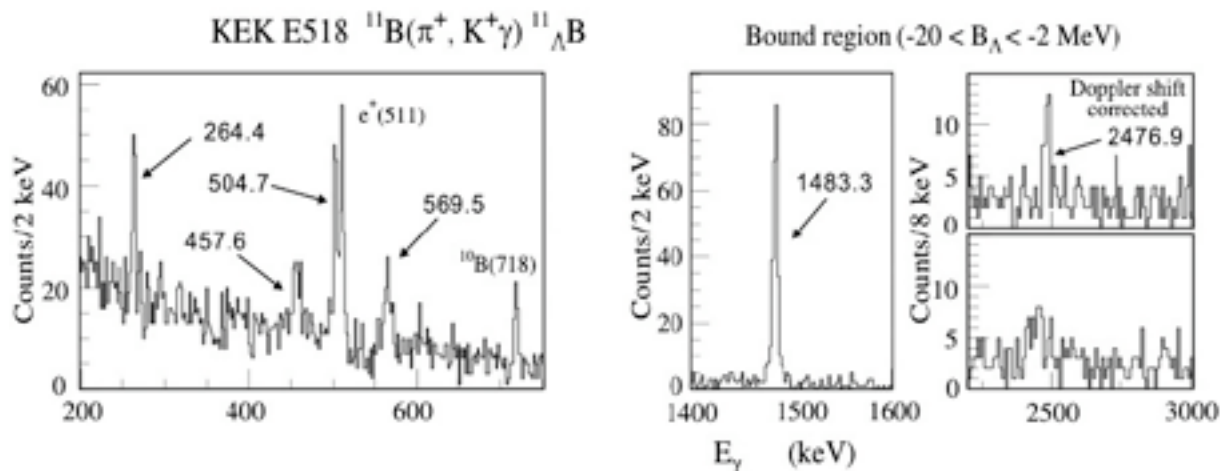


Fig. 4-2-7 The γ ray spectra of $^{11}_{\Lambda}\text{B}$ hypernuclei. Six transitions were observed.

have been successfully observed from $^{11}_{\Lambda}\text{B}$, as shown in Fig. 4-2-7, and their energies and relative yields have been measured. Experiment E521 for the study of neutron-rich Λ hypernuclei used the in-flight (π^-, K^+) DCX reaction on a ^{10}B target in order to produce a $^{10}_{\Lambda}\text{Li}$ hypernucleus for the first time. From the missing-mass spectrum on ^{10}B at 1.2 GeV/c incident momentum, the $^{10}_{\Lambda}\text{Li}$ signal is estimated at 11.3 ± 1.9 nb/sr. The E522 group optionally took (π^-, K^-) data to search for the Θ^+ via $\pi^- p \rightarrow \text{K}^+ \text{X}$ reaction. Scintillation fibers and polyethylene were used as a target. The missing mass spectrum at $P_{\pi^-} = 1.92$ GeV/c (Fig. 4-2-8) shows a bump at around 1.53 GeV/c². Since the statistical significance was not so large, the upper limit of the differential cross section via the (π^-, K^-) reaction was derived as $d\sigma/d\Omega = 3.2$ $\mu\text{b/sr}$ (preliminary) at the 90% confidence level. The E546 group studied the electron rearrangement after formation of pionic atoms by measuring the electronic X rays (eX rays) and pionic X rays emitted from pionic atoms in various elements ranging from zinc to lead. The differences in eX-ray energy between the Z-1 atom and pionic atom for $\text{K}_{\alpha}\text{X}$ rays are smaller than those for K_{β}X rays in the low Z region. The observed phenomena sug-

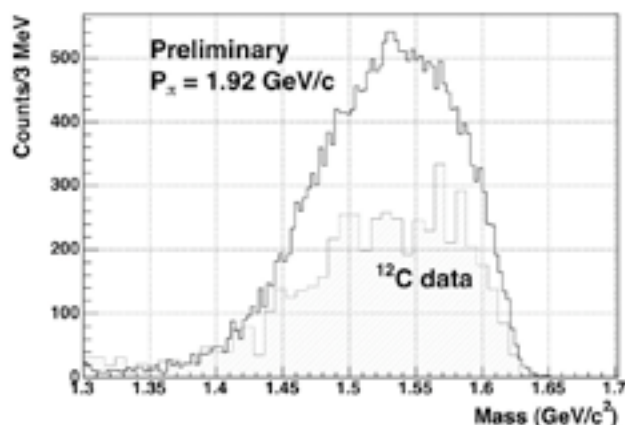


Fig. 4-2-8 Missing mass spectrum of the (π^-, K^-) reaction at $P_{\pi^-} = 1.92$ GeV/c. The hatched histograms are the carbon target data normalized by the target and beam count; these histograms represent the contribution of carbon nuclei in the scintillation fiber and polyethylene target.

gest that pionic atoms are highly ionized by the Auger process during the pionic cascade in the relatively low Z region.

4.3 K2K Experiment

K2K (KEK PS-E362) is the first accelerator-based long-baseline neutrino oscillation experiment from KEK to Kamioka. The main physics goal of K2K is to confirm $\nu_\mu \rightarrow \nu_\tau$ oscillation discovered in atmospheric neutrinos. In addition, K2K has rich physics for the study of other oscillation channels, such as $\nu_\mu \rightarrow \nu_e$ appearance, and neutrino-nucleus interactions in the few GeV region. In FY2004, evidence of neutrino oscillation, namely, the energy-dependent disappearance of muon neutrinos, was published. This result is one of the most important physics goals in K2K, and is described in this report.

An intense muon neutrino beam is produced at the KEK Proton Synchrotron (PS), and this beam is detected at Super-Kamiokande (SK) after traveling 250 km. K2K started data taking in June 1999 and finished in November 2004 with 9.1×10^{19} protons on target (POT) accumulated for analysis. The record of delivered POT to K2K is summarized in Fig. 4-3-1.

In the analysis, we use part of the data collected before February 2004, corresponding to 8.9×10^{19} POT. The neutrino flux and spectrum at KEK are measured by near neutrino detectors: a one kiloton water Cherenkov detector (1KT), a scintillating-fiber/water-target tracker (SciFi), a fully active fine-segmented scintillator tracker (SciBar), and a muon range detector (MRD). The number of interacted neutrinos corresponding to the flux is measured by 1KT with comparably high efficiency to SK. The number of neutrino events in SK without neutrino oscillation is estimated to be 151^{+12}_{-10} based on the neutrino

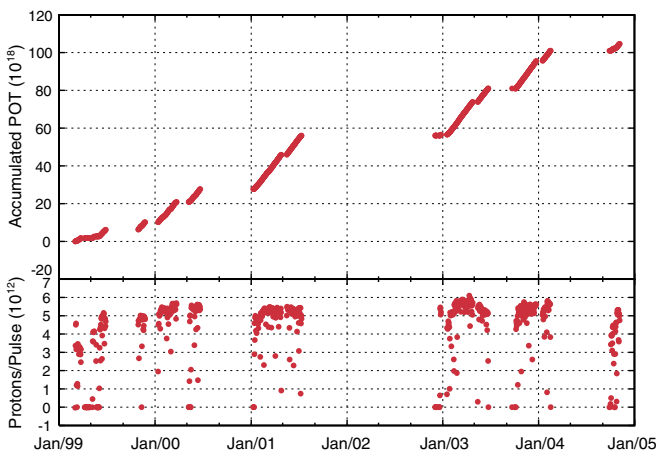


Fig. 4-3-1 Delivered POT and beam intensity per pulse to the K2K experiment from June 1999 to November 2004.

events measured by 1KT. The number of observed neutrino events in SK is 107, as summarized in Table 4-3-1. Thus, we observe a significant deficit of neutrino events in SK, as one of the evidences of neutrino oscillation.

Table 4-3-1 Summary of the SK events. MC is a prediction by Monte Carlo simulation without neutrino oscillation

	Data	MC
Single-ring μ -like	57	85.5
Single-ring e-like	10	8.7
Multi-ring	40	56.7
Total	107	150.9^{+12}_{-10}

The neutrino energy spectrum at KEK is measured by 1KT, SciFi, and SciBar complementarily. The measured neutrino spectrum, which is a product of flux and cross section, is shown in Fig. 4-3-2. The measured spectrum agrees with the prediction of the beam Monte Carlo simulation. The neutrino spectrum at SK is estimated based on the measurement at KEK. In SK, neutrino energy is reconstructed with an assumption of the charged-current quasi-elastic (CCQE) interaction. In order to enhance the fraction of CCQE events, the single-ring μ -like events are selected in SK. Fifty-seven events are selected to

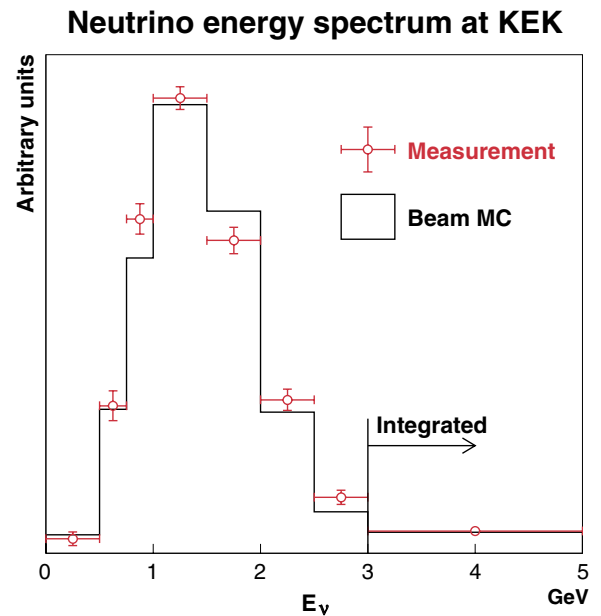


Fig. 4-3-2 Neutrino energy spectrum measured at KEK. The spectrum is a product of flux and cross section.

measure the neutrino energy. The distribution of the reconstructed neutrino energy in SK is shown in Fig. 4-3-3. The observed spectrum does not match the expectation without neutrino oscillation, but matches that with neutrino oscillation.

A two-flavor neutrino oscillation analysis is performed by the maximum-likelihood method. In the analysis, both the number of neutrino events and the energy spectrum shape are used. The best fit point in the physical region is found at $(\sin^2 2\theta, \Delta m^2) = (1.0, 2.8 \times 10^{-3} \text{ eV}^2)$. The allowed regions of the oscillation parameters are shown in Fig. 4-3-4, where the likelihood ratio of each point to the best fit point is evaluated. With neutrino oscillation of the best fit parameters, the expected number of events is 103.8, which agrees with the observation of 107 events. The neutrino energy distribution with the expected distributions of the best fit parameters is also shown in Fig. 4-3-3. The no-oscillation probability is calculated to be 0.0050% (4.0σ). When only normalization (spectrum) information is used, the probability is 0.26% (0.74%). The 90% C.L. contour crosses the $\sin^2 2\theta = 1$ axis at $\Delta m^2 = 1.9$ and $3.6 \times 10^{-3} \text{ eV}^2$, which is consistent with the results from atmospheric neutrinos.

In FY2004, K2K achieved the original goal and confirmed neutrino oscillation. For the oscillation analysis, knowledge of the neutrino-nucleus cross section is improved by the near neutrino detectors: IKT, SciFi, and SciBar. As an improvement, the analysis of SciBar data gives a much smaller cross section of charged-current coherent pion production than the prediction by several models, which resolves the long-standing problem of the forward muon deficit in K2K. More results are expected to appear in FY2005.

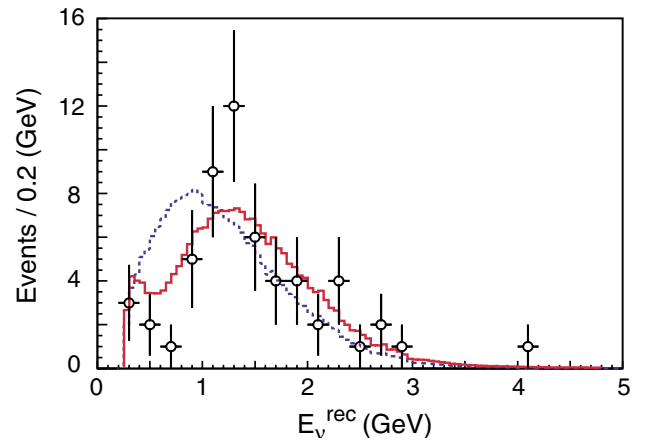


Fig. 4-3-3 Reconstructed neutrino energy distribution of single-ring μ -like events. Points with error bars are data, the solid line is the best fit spectrum with neutrino oscillation, and the dashed line is the expected spectrum without oscillation. These histograms are normalized by the number of observed events (57).

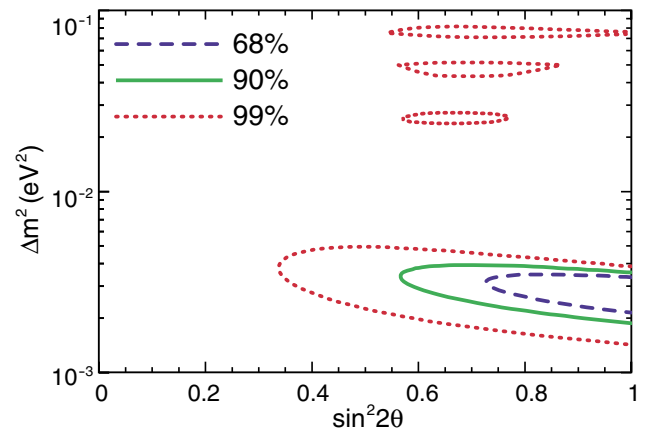


Fig. 4-3-4 Allowed regions of oscillation parameters. The dashed, solid, and dot-dashed lines show the 68.4%, 90%, and 99% C.L. contours, respectively.